ISSN (e): 2250 – 3005 || Volume, 09 || Issue, 7 || July– 2019 ||
International Journal of Computational Engineering Research (IJCER)

Measurement of Velocity Fields Using Hybrid Detectionmethods

Tommaso Tocci[1], Lorenzo Capponi[2], Roberto Marsili[1], Gianluca Rossi[1]
[1]*University of Perugia, Department of Engineering, via G. Duranti 93, 06125 Perugia, Italy,*
[2]*University of Padova, CISAS, Via Venezia 15, 35131 Padova, Italy*
Corresponding Author: Tommaso Tocci

ABSTRACT: *Image analysis techniques such Particle Image Velocimetry or Laser Doppler Velocimetry are usually usedin order to measurevelocity fields. These methods need expensive instrumentation and complex test benchset-ups. In this research an algorithm based on computer vision method Scale Invariant Feature Transform is elaborated in order to evaluate velocity field map in precise and optimized way. Filtering algorithm is used to improve the results. The developed method is applied on a suction system and the obtained speed maps are compared to anemometry measurements. This comparison leads to completely reliable results, both in terms of profile and mean velocity. Uncertainty analysis brings excellent results considering the random nature of its physic.*

KEYWORDS: *Image analysis, Velocity field, Algorithm development, Scale Invariant Feature Transform (SIFT), Detection methods*

Date of Submission: 30-06-2019 Date of Acceptance: 19-07-2019

I. INTRODUCTION

The evaluation of velocity fields is avery researched topic in fluid dynamics. In fact, through them, it is possible to estimate parameters and phenomena, such vorticity, speed and its direction.

Measurements of these quantities is generally carried out by standard image analysismethods [1][2], such as the Particle Image Velocimetry (PIV) [3][4]. Furthermore, techniques based on differentprinciples have been also elaborated for these applications, for example the Laser Doppler Velocimetry (LDV) [5], the Laser Speckle Velocimetry (LSV) [6] and the Digital Particle Image Velocimetry (DPIV) [7]. Moreover, Optical flow methods are usually used in order to build velocity maps [12][13], even ifambiguities, changing lighting conditions and occlusions generally limit the application of this technique.

The aim of this work is to develop a tough algorithm that is able to estimatevapor velocity fields using less complex and expensive instrumentationwith less restrictions on test conditions respect to already mentioned methods. Furthermore, the computer visiontechnique Scale Invariant Feature Transform (SIFT) has been chosen as a working base. It is a feature detection algorithm [14][15][16]used to monitor and describe local features in images[17][18]. However, this method is generallyapplied for different research areas, such in medical field [19], face detection [20], urban planning [21] or in surface topography [22]. In this study a user-friendly application has been developed, based on the SIFT algorithm that is able to measure and to draw velocity fields. Moreover, Random Sample Consensus (RANSAC) filtering algorithm has been necessary for improve the results. The elaborated method has been tested on a suction system. Many different conditions have been analyzed and the results have been compared to an anemometric measurement.

The research is organized as follows: in Section 2 the theoretical background and the algorithm implementation are presented; in Section 3 test bench is defined; in Section 4 results and uncertainty analysis are reported; Section 5 draws the conclusions.

II. ALGORITHM DEVELOPMENT

2.1 SIFT and RANSAC

Scale Invariant Feature Transform (SIFT) is a computer vision algorithm usually used to extract features from an image[17]. It is absolutely invariant from translations, rotations and projective transformations, and partially from changes of illumination and point of view shifts [23].

The algorithm identifies descriptors points that are highly distinct, and therefore it findscorrespondences with high probability, and every feature is represented uniquely by the descriptor.This method has been used in this research in order to detect markers and match keypoints to reconstruct the velocity

field. Moreover, a filtering method has been necessary to obtain better results. Random Sample Consensus has been chosen due to its properties. Random Sample Consensus (RANSAC) is an non-deterministic iterative algorithm for the estimation of parameters of a model, starting from a set of input data containing many outliers [24]. It generates solutions using the minimum number of observations necessary to estimate the parameters of the model.The parameters useful for this type of analysis are the input data, the outliers, the so called “sample set”and “consensus set”.

2.2Matching

In this work, the frame acquired at the instant t_i is called the "PRE" frame and the one extracted at the time $t_i+\Delta t$ is called "POST" frame. The developed method allows to use the SIFT to determine the displacements described by the keypoints, identified between the PRE frame and the POST frame. A map of the velocity of these keypoints is so created. Repeating this operation for all the frames of the video and superimposing the vector maps between each pair of PRE and POST frames, a global velocity field is built using all the keypoints identified.Each frame is subdivided into nine overlapped *Region of Interest* (ROI). The matching phase begins from the first frames pair, with PRE = t_i and POST= $t_i+\Delta t$. The first iteration looks for matching between the ROI 1 of the PRE frame and all the near ROIs and itself in the POST frame, i.e. the ROI 1,2,4,5, then the second iteration looks for matching between the ROI 2 of the PRE frame and all the near ROIs and itself in the POST frame, i.e. the ROI 1,2,3,4,5,6. The iteration is repeated 9 times, one for each ROI of the PRE frame. However, in different ROIs, being overlapped, the same matching can be observed: for this reason, these duplicates are deleted. In the next step, the second frames pair is analyzed (PRE = $t_i+\Delta t$, POST= $t_i+2\Delta t$). The process continues for each pair of frames extracted from the video. As the pairs of frames are processed, a matching matrix is filled out: it contains the x-y coordinates [pixel] of the keypoints of the PRE and POST frames, the displacement and velocity values of the points, as shown in theTable 1.

Table 1 - Matching matrix

# Matching	X_{PRE}	Y_{PRE}	X_{POST}	Y_{POST}	u$[m]$	v$[\frac{m}{s}]$
1	x_{11}	y_{11}	x_{21}	y_{21}	u_1	v_1
2	x_{12}	y_{12}	x_{22}	y_{22}	u_2	v_2
...	...	...	...	...	...	...
n	x_{1n}	y_{1n}	x_{2n}	y_{2n}	u_n	v_n

The setting parameters of the matching phases are the *keypoint threshold* and the *matching threshold*. The first is used in order to avoid non-stable keypoints, so they are selected only if the extremes of the Gaussian function are higher than a threshold value. The second acts when a descriptor D_i is "matched" with a descriptor D_{i+1}, only if the Euclidean distance between $D_i$and D_{i+1} multiplied by the threshold value is not greater than the distance between D_i and all the other descriptors. Results of this phase are two different maps, exposed in**Error! Reference source not found.**.

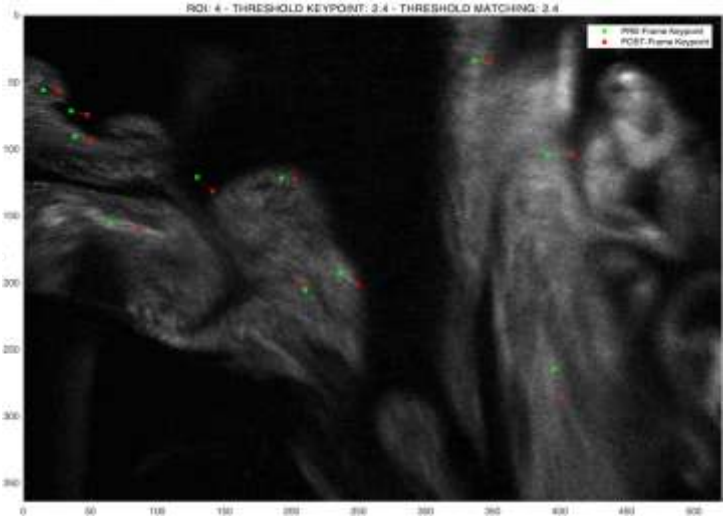

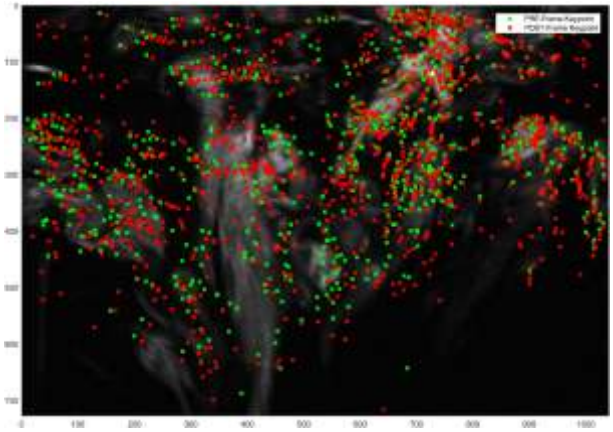

Figure 1 - Matching map on ROI 5 of the first pair of frames (a) Cumulative matching map of all frames (b)

2.3Filtering

In order to limit the number of false matches, the video is acquired with a frame rate as high as possible. False matches can not be deleted upstream, so filtering is necessary in order to discard the majority of failed vectors and build a velocity field as reliable as possible.After the definition of an expected speed range, vectors that do not fit in are filtered, as shown in Figure 2-(b). Subsequently, the mean direction of the vectors within the floating window is determined: each vector with a direction that differs too much from the mean value is then filtered Figure 2-(c).

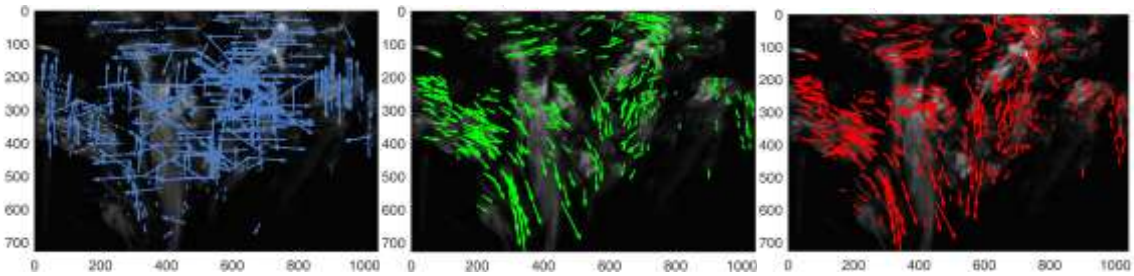

Figure 2 - Comparison of preliminary filtering. No filter (a) Modulus filtering (b) Direction filtering (c)

The finishing filtering phase is based on RANSAC algorithm [24]. The process involves one hundred iterations for each floating window. A new matrix is created, called the *ransac matrix*, which contains all the keypoints identified within the window.

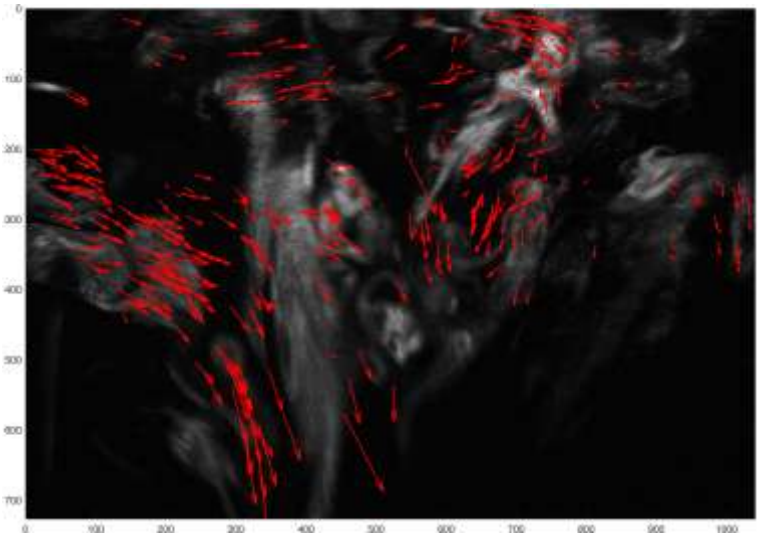

Figure 3 - Output map obtained by finishing filter (RANSAC algorithm)

Finally, the algorithm autonomously creates a 25-pixels mesh grid that is used to determine an interpolated velocity field. In order to have a map as complete as possible, it is therefore necessary to have the highest and most uniform number of real vectors.

III. EXPERIMENTAL ANALYSIS

In this Section the experimental analysis is described, the test bench and the measurement chain are introduced and the experimental setup is presented.

3.1 Test bench

The test bench used in the experimental analysis consists of steam production, suction, illumination, seeding and motion system as well as signal acquisition camera. Test bench model is shown in Figure 4.

The fluid analysed in this experiment is water vapour, and the steam is generated by boiling water inside a pot. The lighting system green laser generator, which produces a laser blade with a 90° opening. The inseminating fluid used is a glycol-water mixture, produced by a proper generator. A tracer is also used[25], due to the reflections and permanence properties better than water vapour. The seeding product is inoculated directly on the analysis plane using a perforated copper tube, adjustable in height.

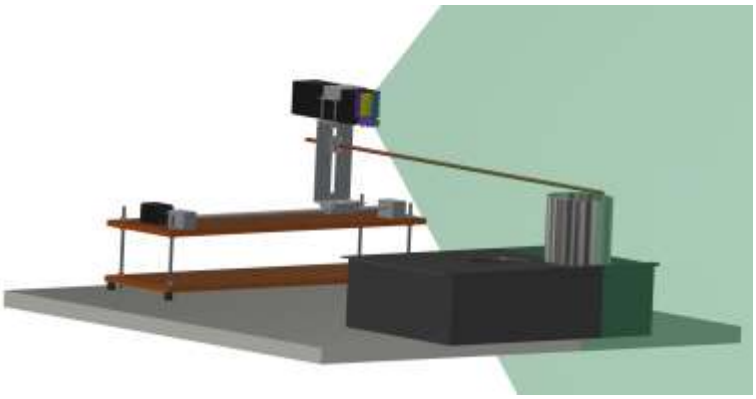

Figure 4 - Test bench model

In order to be able to handle laser blade and insemination system together, the entire system is mounted on a slide driven by a stepper motor. The acquisition system consists of a CCD vision camera (Teledyne DALSA Genie Nano M2450) capable of recording greyscale video with a resolution of 2448x2048 pixels at 90 fps and a 2/3 lens (Chiopt FA1202A) with 1.4 focal opening.

3.2 Experimental setup

The algorithm has been tested in different conditions of use, using diverse receptacles sizes and aspiration speeds of the hood.

A set of 400 frames is acquired for each usage condition, shown in Table 2. The acquisition plane and the positioning of the pots are defined trying to limit shadows and interferences.

Table 2 - Experimental setup

Test Number	Number of Pot	Type of Pot	Aspiration Speed
1	1	High	3
2	1	High	6
3	1	High	9
4	1	Low	3
5	1	Low	6
6	1	Low	9
7	2	High	3
8	2	High	6
9	2	High	9

3.3 Anemometric measurement

Measurement has been performed using a hot-wire anemometry in order to validate the results obtained by the algorithm. A grid of acquisition points has been defined and measurements are repeated for different

speeds of the suction system. Speed values are determined by arithmetic mean of all measuredvalues and,interpolating the data, the complete speed map is given, as shown in the Figure 5.

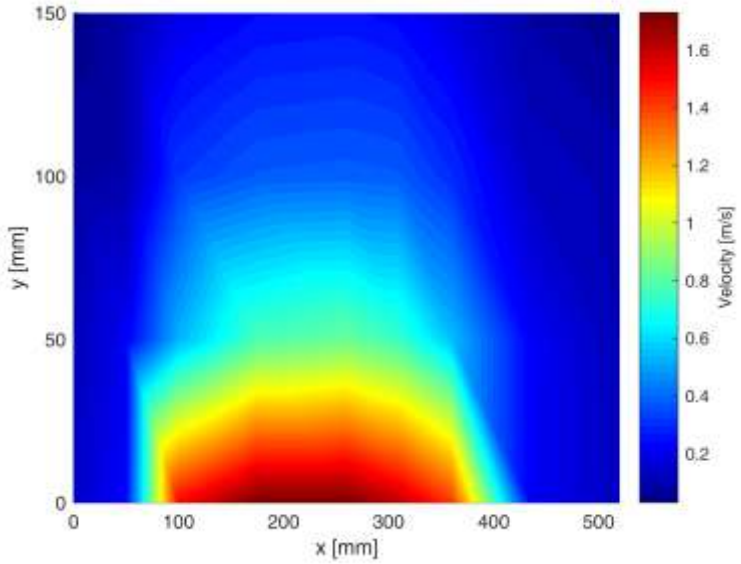

Figure 5 - Interpolated anemometric velocity map

IV. RESULTS

The interpolated velocity field map has been extracted from the filtering algorithm and it is shown in Figure 6.

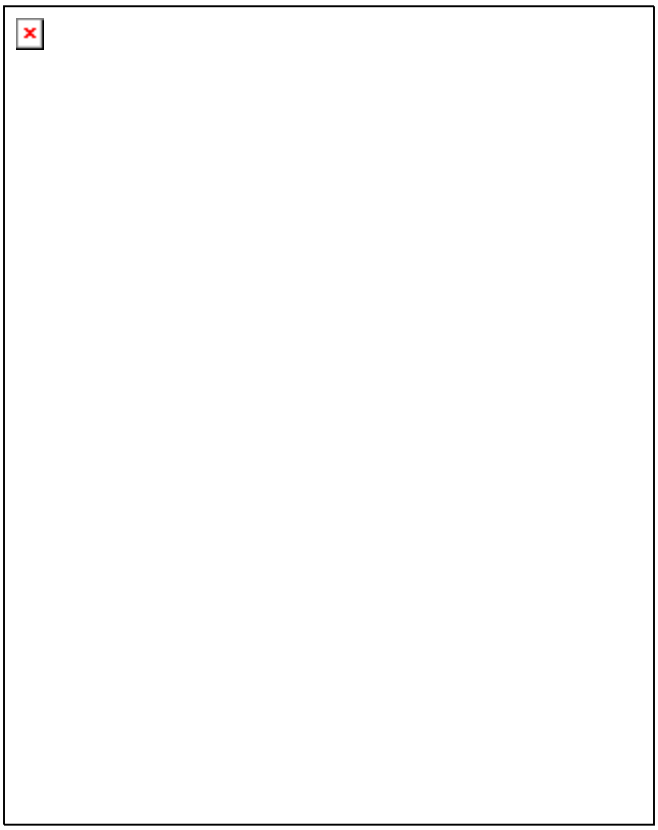

Figure 6 - Interpolated Velocity Field - Test 2

In order to verify the reliability of the developed method and validate the velocity maps, a comparison between the speed profiles obtained with algorithm and hot-wire anemometer has been done.

The analysis in a plane that is 82.5 mm from suction plane is shown inFigure 7.

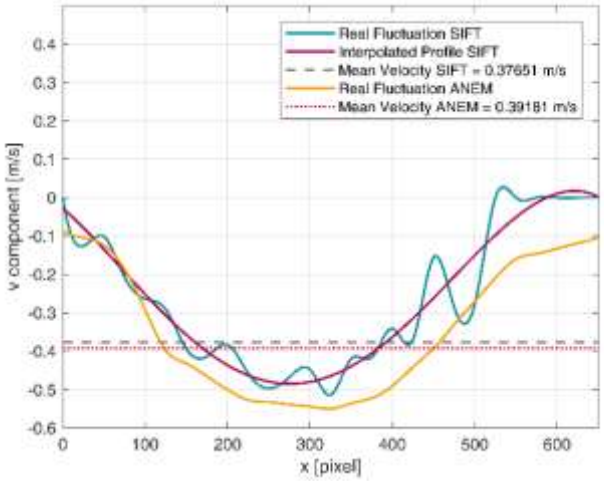

Figure 7 - Test 2 - Comparison between velocity profiles extracted in the distant plane

The fluctuation of the velocity obtained with the image analysis is due to the turbulence caused by convective phenomena triggered by the fluid. This fluctuation cannot be measured by anemometry because the map is obtained by means of average punctual speed measurements.For this reason, the comparison with the anemometer has been done in term of velocity values and interpolated SIFT profile of the real fluctuation. Then analyzing these parameters, it can be clearly seen that the profiles are almost perfectly superimposable. Same goes for mean velocity and for other test conditions.

5.1 Uncertainty analysis

Uncertainty analysis on the measurement has been also performed: five measurements were carried out on the same test with a fixed set-up condition. The velocity values at 57.5 mm from the profile are extracted and reported in Table 2.

Table 2 – Experimental velocity measurement for uncertainty

	Measurement #1	Measurement #2	Measurement #3	Measurement #4	Measurement #5
x [pixel]	v $[\frac{m}{s}]$	v $[\frac{m}{s}]$	v $[\frac{m}{s}]$	v $[\frac{m}{s}]$	v $[\frac{m}{s}]$
125	0,49870	None	None	None	None
150	0,66490	0,62800	None	None	0,58210
175	0,81940	1,04800	0,88120	0,68360	0,64980
200	1,08580	1,01340	0,85960	0,80060	1,01800
225	0,98550	1,21210	0,95140	0,93740	1,10160
250	1,03750	0,99860	1,16390	1,02110	1,10870
275	1,05360	1,22130	1,16130	1,03100	1,04340
300	1,06640	0,97570	1,04570	1,12400	0,94190
325	0,97140	0,97750	1,03100	1,14810	0,96800
350	1,02720	1,22900	1,08760	1,05950	1,08940
375	1,03910	1,19970	1,18460	1,19540	1,25410
400	0,99700	None	None	None	None

Subsequently, in order to have denser measurements, a grid of spatial coordinates has been defined in x [pixels]. However, where a value is missing, a velocity value obtained by interpolation with spline starting from the known speed values is inserted. The cumulative map is then built with the complete velocity fluctuation for each measurement, as shown in Figure 8.

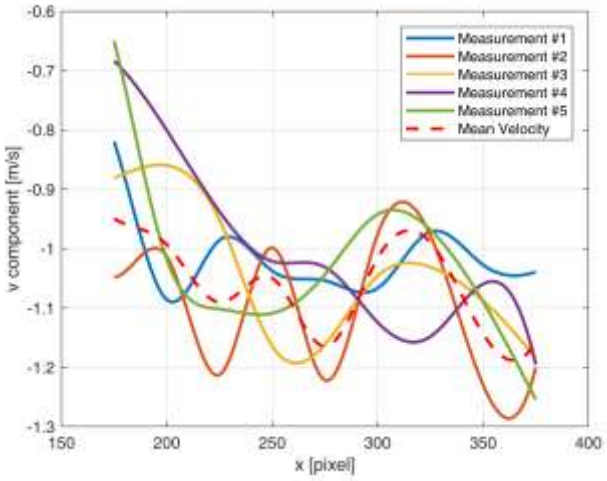

Figure 8 - Velocity fluctuation of 5 different measure for determine the uncertainty - Test 2

The uncertainty analysis of measurement has been perfomedusing the UNI CEI 13005 [26]. The uncertainty value results in 4.05%.

V. CONCLUSION

The objective of the work was to develop a hybrid image analysis algorithm, based on feature detection methods, that is able to measure and estimate vapour velocity field. Scale Invariant Feature Transform has been chosen as starting point. However, this method was born for completely different research topic. Developed algorithm has been tested on a suction system and after software implementation, experimental analysis has been performed. Frames have been acquired in different operating conditions, in order to simulate a complete usage of the system. Maps of velocity field have been evaluated and they have been compared to those given by hot-wire anemometry measurements. Outcomes given by anemometry and by SIFT-based algorithm are totally comparableboth in terms of profile and mean velocity. Moreover, an uncertainty analysis of the measures obtained from the algorithm has been performed. Results are reliable because theyshow relatively low uncertainty considering the hard-operating conditions.

REFERENCES

[1]. E. Speranzini, R. Marsili, M. Moretti, and G. Rossi, "Image analysis technique for material behavior evaluation in civil structures," *Materials (Basel).*, vol. 10, no. 7, p. 770, 2017.
[2]. F. Bianconi *et al.*, "Comparison between two non-contact techniques for art digitalization," in *Journal of Physics: Conference Series*, 2017, vol. 882, no. 1, p. 12005.
[3]. M. Raffel, C. E. Willert, F. Scarano, C. J. Kähler, S. T. Wereley, and J. Kompenhans, *Particle image velocimetry: a practical guide*. Springer, 2018.
[4]. J. Mizeraczyk *et al.*, "Measurements of the velocity field of the flue gas flow in an electrostatic precipitator model using PIV method," *J. Electrostat.*, vol. 51, pp. 272–277, 2001.
[5]. F. Durst, "Principles of laser Doppler anemometers," in *In Von Karman Inst. of Fluid Dyn. Meas. and Predictions of Complex Turbulent Flows, Vol. 1 11 p (SEE N81-15263 06-34)*, 1980, vol. 1.
[6]. R. Meynart, "Instantaneous velocity field measurements in unsteady gas flow by speckle velocimetry," *Appl. Opt.*, vol. 22, no. 4, pp. 535–540, 1983.
[7]. C. E. Willert and M. Gharib, "Digital particle image velocimetry," *Exp. Fluids*, vol. 10, no. 4, pp. 181–193, 1991.
[8]. M. Becchetti, R. Flori, R. Marsili, and G. L. Rossi, "Measurement of stress and strain by a thermocamera," in *Proceedings of the SEM Annual Conference*, 2009.
[9]. R. Marsili, G. Rossi, and E. Speranzini, "Study of the causes of uncertainty in thermoelasticity measurements of mechanical components," *Measurement*, vol. 118, pp. 230–236, 2018.
[10]. F. Cannella, A. Garinei, R. Marsili, and E. Speranzini, "Dynamic mechanical analysis and thermoelasticity for investigating composite structural elements made with additive manufacturing," *Compos. Struct.*, vol. 185, pp. 466–473, 2018.
[11]. R. Marsili, G. Rossi, and E. Speranzini, "Fibre Bragg Gratings for the monitoring of wooden structures," *Materials (Basel).*, vol. 11, no. 1, p. 7, 2018.
[12]. B. K. P. Horn and B. G. Schunck, "Determining optical flow," *Artif. Intell.*, vol. 17, no. 1–3, pp. 185–203, 1981.
[13]. G. Allevi, L. Casacanditella, L. Capponi, R. Marsili, and G. Rossi, "Census Transform Based Optical Flow for Motion Detection during Different Sinusoidal Brightness Variations," in *Journal of Physics: Conference Series*, 2018, vol. 1149, no. 1, p. 12032.
[14]. S. Logozzo, M. Valigi, and G. Canella, "Advances in Optomechatronics: An Automated Tilt-Rotational 3D Scanner for High-Quality Reconstructions," in *Photonics*, 2018, vol. 5, no. 4, p. 42.
[15]. M. C. Valigi, S. Logozzo, and G. Canella, "A Robotic 3D Vision System for Automatic Cranial Prostheses Inspection," in *International Conference on Robotics in Alpe-Adria Danube Region*, 2017, pp. 328–335.
[16]. M. C. Valigi, S. Logozzo, and G. Canella, "A new automated 2 DOFs 3D desktop optical scanner," in *Advances in Italian Mechanism Science*, Springer, 2017, pp. 231–238.

[17]. D. G. Lowe, "Object recognition from local scale-invariant features," in *iccv*, 1999, p. 1150.
[18]. T. Lindeberg, "Scale-space theory: A basic tool for analyzing structures at different scales," *J. Appl. Stat.*, vol. 21, no. 1–2, pp. 225–270, 1994.
[19]. W. Cheung and G. Hamarneh, "N-sift: N-dimensional scale invariant feature transform for matching medical images," in *2007 4th IEEE International Symposium on Biomedical Imaging: From Nano to Macro*, 2007, pp. 720–723.
[20]. M. Bicego, A. Lagorio, E. Grosso, and M. Tistarelli, "On the use of SIFT features for face authentication," in *2006 Conference on Computer Vision and Pattern Recognition Workshop (CVPRW'06)*, 2006, p. 35.
[21]. D. Pagliari, "Rilievo di traiettorie urbane con approccio fotogrammetrico: una sperimentazione orientata all'automazione," 2011.
[22]. M. Moretti, G. Gambucci, R. K. Leach, and N. Senin, "Assessment of surface topography modifications through feature-based registration of areal topography data," *Surf. Topogr. Metrol. Prop.*, vol. 7, no. 2, p. 25003, 2019.
[23]. R. Szeliski, *Computer vision: algorithms and applications*. Springer Science & Business Media, 2010.
[24]. M. A. Fischler and R. C. Bolles, "Random sample consensus: a paradigm for model fitting with applications to image analysis and automated cartography," *Commun. ACM*, vol. 24, no. 6, pp. 381–395, 1981.
[25]. A. Melling, "Tracer particles and seeding for particle image velocimetry," *Meas. Sci. Technol.*, vol. 8, no. 12, p. 1406, 1997.
[26]. U. N. I. CEI, "13005," *Guid. all'espressione dell'incertezza di misura (ex UNI CEI 9)*.

Tommaso Tocci " Measurement of Velocity Fields Using Hybrid Detectionmethods" International Journal of Computational Engineering Research (IJCER), vol. 09, no.7, 2019, pp 13-20